

Received: 14 February 2024 / Accepted: 19 March 2024 / Published online: 20 March 2024

*milling, force estimation,
friction modeling*

Adrian Karl RÜPPEL^{1*},
Markus MEURER¹,
Thomas BERGS^{1,2}

A NEW GREY BOX APPROACH FOR FRICTION MODELLING OF MACHINE TOOL DRIVES

Measurement of the process force in milling is usually conducted by using piezo-electric dynamometers which are costly and reduce the stiffness of the system. A less invasive alternative is an indirect estimation of cutting forces based on the power of the servo drives. However, a correction of frictional effects from the transmission system is necessary to achieve accurate results. Most machine tools are equipped with ball-screw drives whose friction behavior is highly nonlinear due to dependency on both velocity and position. This study provides a novel approach to consider all frictional and inertial effects in transmission behavior of ball-screw drives by utilizing the well-established generalized MAXWELL slip (GMS) model and combines it with a data-based approach, namely support vector regression (SVR). The approach acquires the internal states of the GMS model and uses them as an additional input for the SVR. The model is validated on different experiments conducted on a five-axis machining center and compared to established friction models, as well as a sole SVR. The results show the model to have errors between 7% and 12% over the full working range of the x- and y-axes, respectively, outperforming the benchmark models significantly.

1. INTRODUCTION

Cutting processes are characterized by extreme conditions regarding temperature, rate of forming, and process force. Especially the latter is one of the key measures when monitoring cutting processes. Due to high loads and dynamics, accurate measurement of cutting forces requires mostly piezo-electric dynamometers or strain-gauges to date, both of which are costly and reduce the stiffness of the system, increasing the risk for process instabilities. Alternative ways of indirectly measuring the process force are, therefore, an important research field at present.

A promising way of indirectly measuring the process force is by utilizing the proportionality of motor currents and motor torque, both of which are directly proportional, allowing the estimation of the axis load without sophisticated signal processing. However, the friction

¹ Manufacturing Technology Institute (MTI), RWTH Aachen University, Germany

² Fraunhofer Institute for Production Technology (IPT), Germany

* E-mail: a.rueppel@mti.rwth-aachen.de

<https://doi.org/10.36897/jme/186269>

in the transmission system of the machine tool disturbs the forces and complicates the current-based measurement of the forces acting in the cutting process. Especially ball-screw drives, which are widely used in the auxiliary axes of milling machine tools, have a highly nonlinear frictional behavior, and necessitate the usage of more complex signal processing techniques.

This work introduces a new grey box approach for modeling friction in machine tool drives, utilizing physically motivated friction as well as machine learning models and combines them to increase accuracy. The personal motivation is a current-based force estimation to be used in a model predictive force control for milling which has been developed using piezo-electric force dynamometers [1–2]. However, the predominant field to compensate for friction in machine tool drives is precision machining (e.g. [3–6]), where the model could also be utilized. The work is structured as follows: Chapter 2 provides an overview of the state-of-the-art in modeling friction with focus on machine tool drives. In Chapter 3 the grey box modeling approach is described. The experimental setup is laid out in Chapter 4. Validation of the new model and comparison to established friction models is provided in Chapter 5. The work ends with a conclusion in Chapter 6.

2. STATE-OF-THE-ART

Friction is highly dependent on the surfaces in contact. In technical systems within machines usually metal-to-metal contact is predominant. Therefore, the explanations in this work are limited to this kind of frictional system. Armstrong-Hélouvry et al. give an excellent overview over frictional phenomena within technical systems as well as ways to compensate for them [7]. On microscopic level, all surfaces are rough and full of asperities. The actual contact takes place at points where asperities of both surfaces meet. Without relative motion between the two surfaces the asperities will interlock leading to a counter-reactive force against any movement. This is called sticking. When the tangential force between the surfaces becomes too high the asperities break away and the surfaces begin to move. At this point sliding occurs. The frictional force during sliding is generally lower than during sticking and in many dry scenarios friction even decreases with higher velocities [7].

However, to reduce frictional forces and extend life of the components involved technical systems are usually lubricated with oil or grease. In lubricated systems a fluid is separating the surfaces and viscous friction occurs, where higher velocities lead to higher frictional forces [7]. Due to design and cost reasons, technical systems are usually hydrodynamic; regarding lubrication, this means that the fluid film is not existent during stand still and only builds up at a minimum relative velocity [7]. Underneath this velocity threshold viscous friction gets marginal and other frictional behavior occurs. Especially the transition phase from standing dry friction to high velocity moving friction is challenging for friction modeling in technical systems [7].

Depending on relative velocity, the frictional behavior can be split in four regimes: Static (1), boundary lubrication (2), partial fluid lubrication (3), and fluid lubrication (4) [7]. Static (1) friction is characterized by elastic deformation of the interlocking asperities resulting in spring-like behavior. The junction break when the force exceeds the static frictional force also referred to as the Dahl effect. At very small velocities, i.e. in the boundary

lubrication regime (2), no fluid film has built up, yet, leading to solid-to-solid contact and, therefore, solely dry friction occurs. When the velocity increases, partial fluid lubrication (3) occurs, where a fluid film builds up. Viscous lubrication gets predominant; however, some asperities are higher than the fluid film's thickness, leaving a minor solid-to-solid friction left. The last regime, fluid lubrication (4), describes sole viscous friction, where the fluid film is high enough to fully separate the surfaces.

Friction models can be distinguished into two categories: Static and dynamic models. Static models, also referred to as classic friction models, describe the friction force solely depending on the current velocity or normal force. The most basic model is the Coulomb friction model [8], where friction force is only dependent on the normal force and a friction parameter. Viscous friction, which foundation was described by Reynolds [9] and Sommerfeld [10] and worked out by Hersey et al. [11], describes friction force as a function of velocity. Early models assumed a proportional relationship. However, in the above-mentioned hydrodynamic scenarios these models are limited. Stribeck first tried to account for nonlinear behavior at low velocities and described friction by the well-known Stribeck curve [12]. The Stribeck friction model is still widely used up today.

All static models struggle on describing friction behavior at very low velocities. Here, the slow break-away of the asperities result in three phenomena: stiction, stick-slip and frictional lag or frictional memory. Stiction and stick-slip are caused by interlocking asperities and can be described as spring-like behavior, firstly introduced by Dahl (cf. Dahl effect) [13]. Frictional lag refers to a delay between velocity change and friction force and is the reason for hysteresis effects in friction [7]. This phenomenon was described e.g. by Rabinowicz et al. [14]. Hess and Soom measured the lag to be within 3 to 9 ms [15].

To account for these phenomena, dynamic models were introduced, where the friction force is not only related to the current velocity, but also to internal system states. Dahl described the spring-like behavior by modeling a mass spring element and assuming friction to be a function of displacement [13]. However, the Dahl model is lacking the Stribeck effect, assuming only Coulomb friction. Canudas de Wit et al. changed this by introducing the Lund-Grenoble (LuGre) model and combined the Dahl and Stribeck approaches [16]. An essential shortcoming of this model was the lack of describing the nonlocal memory character of friction in the presliding regime. A first approach to overcome this was called Leuven model, which did incorporate the transition effects, but resulted in a very complicated implementation method [17]. Consequently, Al-Bender et al. tried to overcome both problems by utilizing the Maxwell-slip model, where more than one mass-spring element was modeled (see. Fig. 1), and enhanced it to describe both, dry and viscous friction regimes as well as the transient zone [18]. They named it generalized Maxwell-slip (GMS) model. Relating to physical friction models, it is considered state of the art. Data-based approaches are an interesting new field, but not used very often for friction modeling to date. Schwenzer et al. used a support vector regression (SVR), showing the potential of the method [19]. Support vector machines were first introduced by Boser et al. [20] and Vapnik et al. [21] and are capable of describing an arbitrary function with relatively small number of free parameters, making them less prone to model overfitting than other machine learning models.

All previously mentioned friction models assume homogeneous conditions along the full range of motion of the system. In machine tool axes, however, the frictional forces are

strongly dependent on the position of the axis, as can be seen in e.g. [22]. This is mainly caused by the nonlinearity of ball-screw drives [23].

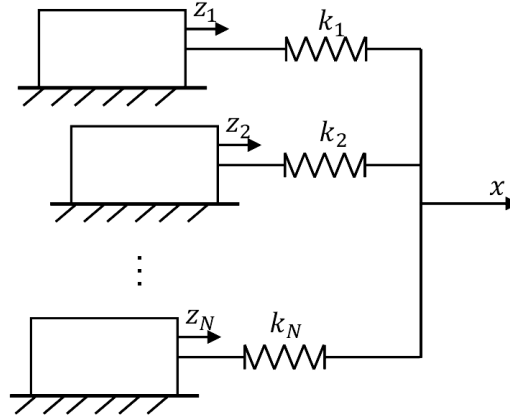


Fig. 1. Depiction of the Maxwell-slip friction model (based on [18])

One way to reduce frictional effects in machine tools are design measures like aero-static bearings [24–25] or magnetic guidances [26–27]. Another way to account for the positional effects is by performing an air cut and subtracting the measured currents, which is an often applied technique in works correcting motor currents (e.g. 28–30). XI et al., for example, used the LuGre model and extended it by a look-up table to account for positional effects [31]. However, the more generic solution is modeling the positional effect and including it into the frictional model. Schwenzer et al. fit a hyperbolic function to account for positional effects [19]. The model provides good results when combined with an SVR, however, it also needs careful training data preparation.

A grey box approach for modeling position and temperature dependency in industrial robots was done by Carlson et al. which used a Radial Basis Function Network (RBFN) for modeling positional effects [32].

3. GREY BOX APPROACH TO MODEL FRICTION OF MACHINE TOOL AXES

The grey box approach proposed in this work splits the total motor current $I_{q,gms}$ into two separate effects

$$I_{q,gms}(a, v) = I_I(a) + I_{fric,gms}(v), \quad (1)$$

with I_I describing the current resulting from inertial effects and $I_{fric,gms}$ describing the current resulting from friction. To prevent any influence from the process only air cuts are performed. p , v and a describe the position, velocity, and acceleration of the axis, respectively. Inertial effects are described by Newtons first law

$$I_I(a) = Ja. \quad (2)$$

The parameter J can be interpreted as moment of inertia of the full transmission system, while a is the acceleration of the axis. The frictional current depends on the velocity v . To

account for velocity effects, the GMS model in the formulation as in Al-Bender et al. is utilized [18]. Tjahjowidodo et al. showed, that it yields the best results in modeling the pre-sliding regime of machine tools [33]. Essentially, the friction is described by N single mass-spring elements i , with the internal states z_i . When sticking, the state equation of each element is given by

$$\frac{dz_i}{dt} = v, \quad (3)$$

and the element remains sticking until the state exceeds the maximum $z_{i,max} = s_i(v)$. When the element is sliding, the state equation is given by

$$\frac{dz_i}{dt} = \text{sgn}(v)C_i \left(1 + \frac{z_i}{s_i(v)}\right). \quad (4)$$

The element keeps sliding until the velocity goes through or approaches zero. The parameter C_i is an attraction parameter, which determines how fast z_i converges to $s_i(v)$. The $\text{sgn}(v)$ or sign function is defined as

$$\text{sgn}(v) = \begin{cases} +1, & \text{for } v > 0, \\ 0, & \text{for } v = 0, \\ -1, & \text{for } v < 0, \end{cases} \quad (5)$$

while $s_i(v)$ describes the velocity weakening function by Stribeck. There are different mathematical formulations for the Stribeck curve; this work uses the formulation by Zschack et al. [34].

$$s_i(v) = s_{\infty,i} + (s_{0,i} - s_{\infty,i}) \cdot e^{-\frac{|v|}{v_{s,i}}}, \quad (6)$$

with the Stribeck velocity $v_{s,i}$, the start value $s_{0,i} = s(v = 0)$ and the end value $s_{\infty,i} = s(v = \infty)$ of each element.

The friction current $I_{\text{fric,gms}}$ is determined by adding all elements up as well as adding a term for viscoelastic effects and for viscous effects, respectively. The equation is given by

$$I_{\text{fric,gms}}(v) = \sum_{i=1}^N (k_i \cdot z_i + \sigma_i \cdot \dot{z}_i) + \mu \cdot v, \quad (7)$$

where k_i is the spring stiffness of each element, σ_i is the viscoelastic parameter and μ is the viscous friction parameter. To reduce the number of parameters that need to be identified, all elements are assumed to have the same velocity weakening function $s(v)$, only scaled by a parameter α_i , resulting in $s_i = \alpha_i s(v)$ as the authors of the original model suggest it [18]. The same is done for $C_i = \alpha_i C$ and $\sigma_i = \alpha_i \sigma$. Furthermore, the authors also suggest, that a total of $N = 4$ elements is enough, which has been followed by in this work as well.

The only input to the GMS model is the velocity, lacking any information of positional dependency on the friction. To account for position as well, the model gets extended by an SVR, which is used as a positional correction method for the previously determined, velocity dependent friction induced current $I_{\text{q,gms}}$ which already includes inertial effects.

Additional to the position p and $I_{q,gms}$ the SVR also takes the vector of internal states $\mathbf{z} = (z_1 z_2 z_3 z_4)$ of the GMS model as an extra input. The output of the SVR is the corrected motor current

$$I_{q,gmssvr}(p, v, a) = f(p, I_{q,gms}, \mathbf{z}). \quad (8)$$

The model will be further called GMSSVR, to distinguish it from a sole SVR. The model is benchmarked against a GMS model, as well as an SVR with the inputs p and v which is given by

$$I_{q,svr}(p, v, a) = f(p, v) + I_l(a), \quad (9)$$

as well as a Stribeck model. An overview of the connections between all models are shown in Fig. .

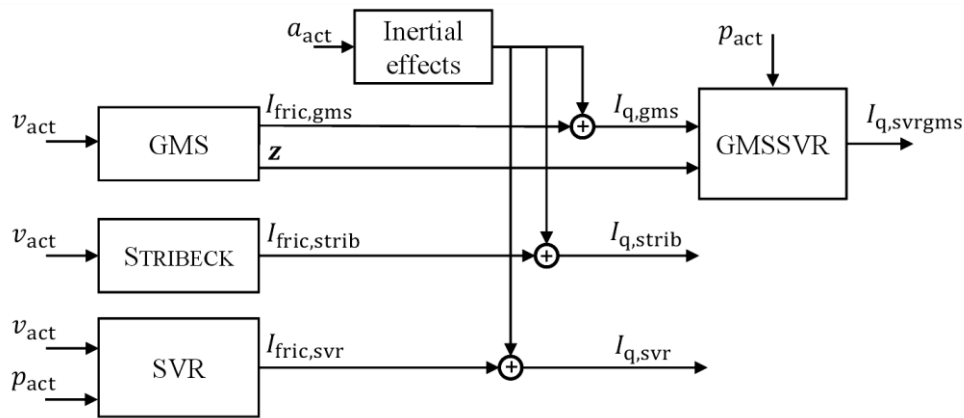


Fig. 2. Overview of the connections between all models. The models are further described in the text

4. EXPERIMENTAL SETUP AND MODEL IDENTIFICATION

This section presents the experimental setup, an overview of the conducted experiments as well as the implementation of the proposed models. Furthermore, the identification procedure with the different data sets is described.

4.1. EXPERIMENTAL SETUP

All experiments were conducted on a Mazak VARIAXIS i-600 5-axis machining center with a Siemens SINUMERIK 840D sl numerical control (NC) unit. To obtain the process signals in real-time the Axis Data Stream (ADAS) NC-feature was used. This configured the NC-kernel to send signals with a sample rate of 500 Hz to a compact Rio (cRio) edge computer by National Instruments.

For manipulating the feed and spindle speed of the machine tool, the cRio sent a signal via OPC Unified Architecture (OPC UA) protocol to the NC-controller. To avoid temperature effects, all axes have been moved for 20 min prior to the experiments, which has been shown as enough to reach a steady state in previous experiments. No lubrication impulse was given during the experiments.

Four datasets have been acquired to train the models, two for the X- and two for the Y-axis respectively. Only one axis was moved at a time. To account for velocity and acceleration dependent effects, experiments with varying velocities in random steps and sinusoidal movement in the middle of the working area of the machine tools axes were conducted. Additionally, experiments were conducted over full working range. For testing the models, an additional random step experiment as well as a full positional range experiment have been conducted. An overview of all datasets is provided in Table 1. The training and test datasets are mutually exclusive.

Table 1. Overview of all datasets

	Dataset	Axis	Strategy	Velocity / mm min^{-1}	Position / mm
Training	A	X	Random steps, sinusoidal	100 – 2000	–225 – –275
		Y	Random steps, sinusoidal	100 – 2000	–425 – –475
	B	X	Constant	600; 1800	–510 – 0
		Y	Constant	600; 1800	–910 – 0
Testing	C	X	Random steps, sinusoidal	100 – 2000	–225 – –275
		Y	Random steps, sinusoidal	100 – 2000	–425 – –475
	D	X	Constant	1200	–510 – 0
		Y	Constant	1200	–910 – 0

4.2. IMPLEMENTATION AND IDENTIFICATION PROCEDURE

To implement the GMS model, a discretization using the forward Euler method has been performed. With the sample time $T = 2$ ms, the discretized model is given by

$$z_{i,k+1} = z_{i,k} + v T, \quad (10)$$

for sticking and by

$$z_{i,k+1} = z_{i,k} + \text{sgn}(v) T C_i \left(1 - \frac{z_{i,k}}{s_i(v)} \right), \quad (11)$$

for sliding. To train the full grey box model a two-step parameter identification was performed. To account for the positional effects as well, the parameters of the GMS model were identified using dataset A, which covers specific velocity dependent frictional effects, the GMSSVR model using dataset B, which covers specific positional effects. Datasets C and D were used for testing. To provide the same prerequisites the benchmark models GMS, SVR and Stribeck were trained using both datasets A and B. The hyperparameters of the SVR and GMSSVR were optimized using bayesian optimization and are shown in Table 2.

Table 2. Optimized Hyperparameters for the SVR and GMSSVR models fit with datasets A and B

	X-axis			Y-axis		
	Kernel	ϵ	C	Kernel	ϵ	C
SVR	Gaussian	0.019	15.2	Gaussian	0.22	9.08
GMSSVR	Gaussian	0.14	18.0	Gaussian	0.32	0.68

5. RESULTS

To validate the models two separate evaluations have been conducted. At first, the models were trained by using only dataset A and tested by only using dataset C with almost negligible positional effects due to limited operating range. Stribeck, GMS and SVR were benchmarked against each other. For all models the root mean squared error (RMSE) and the relative error (RE) were used as metrics according to the equations

$$RMSE = \sqrt{\sum_{n=1}^N \frac{(\hat{I}_n - I_n)^2}{N}}, \text{ and} \quad (12) \quad RE = \frac{RMSE}{\bar{I}}. \quad (13)$$

The estimated value of I is denoted as \hat{I} , the mean of all observed I is denoted as \bar{I} with the total number of observations N . Fig. 3 shows the absolute error $|\Delta I_{act}|$ of all models on the dataset with negligible positional effect (Dataset C), the RMSE and RE are shown in Table 3.

Table 3. RMSE and RE of all models on Datasets A and C (negligible positional effect)

Dataset	Metric	x-axis			y-axis		
		STRIBECK	SVR	GMS	STRIBECK	SVR	GMS
A (Training)	RMSE (in A)	0.09	0.09	0.1	0.13	0.12	0.12
	RE (in %)	9.2	9.2	9.9	13.2	12.2	12.1
C (Testing)	RMSE (in A)	0.13	0.14	0.13	0.15	0.15	0.14
	RE (in %)	11.4	12.6	11.9	14.9	14.4	13.4

All models perform well on the datasets A and C with relative errors between 9.2% and 14.9%. The Stribeck model establishes the best results on X-axis while the GMS model is best on the Y-axis.

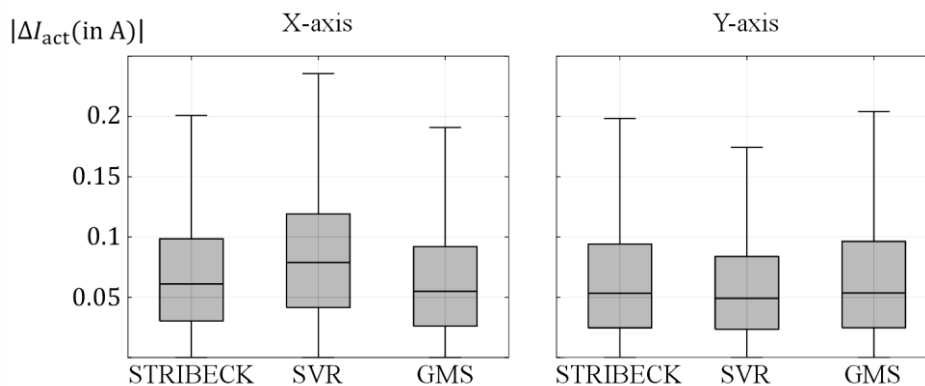


Fig. 3. Absolute error of Stribeck, SVR and GMS models of X- and Y-axis on dataset C. The horizontal bar within the boxes depicts the median; upper and lower edges of the boxes are the upper and lower quartile; the whiskers include 95% of all data; outliers are not depicted

Fig. 4 shows all models compared to the measurement at a section of dataset C. All models have minor errors during acceleration and deceleration phases, especially when the direction is changing. However, the GMS model shows significant advantage during directional changes as it is the only one covering frictional lag and frictional memory effects.

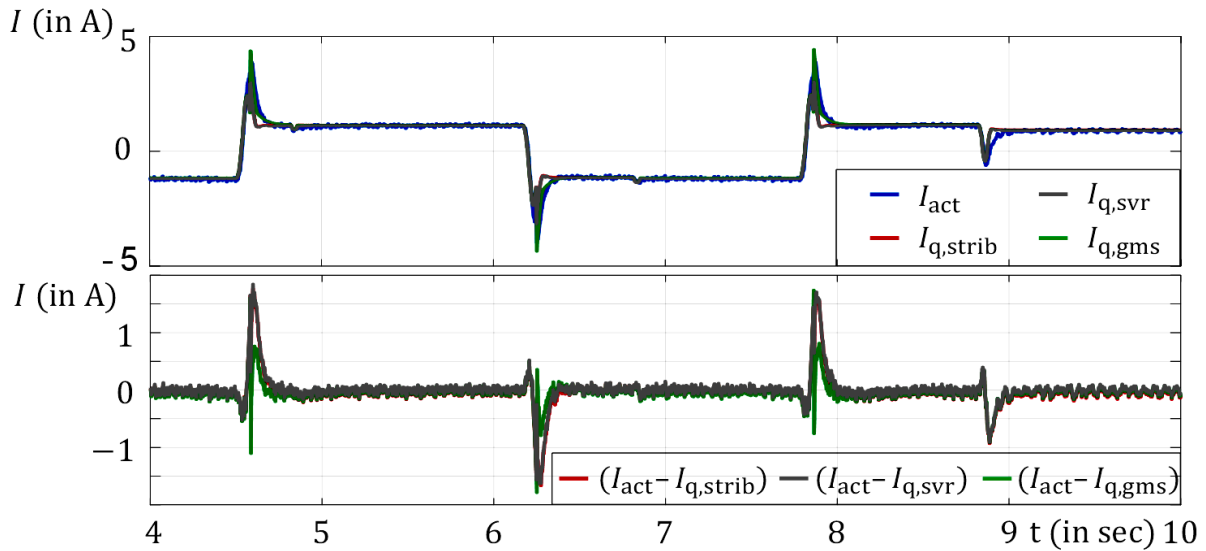


Fig. 4. Comparison of the different models on y-axis in time domain on dataset C (negligible positional effect)

The second model validation was performed using all four datasets, adding positional effects to the data. The Stribeck, GMS and SVR model were all trained by using datasets A and B together. For the GMSSVR model, the two step identification procedure explained in section 4.2 was performed. The results on the test datasets (C and D) are shown in Fig. , RMSE and RE of all data is given in Table 4.

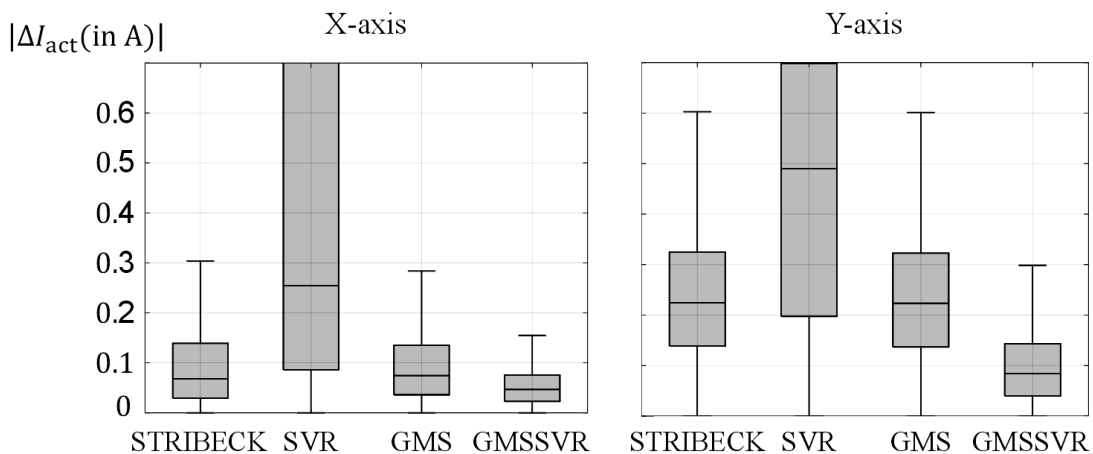


Fig. 5. Absolute error of Stribeck, SVR, GMS and GMSSVR models of X- and Y-axis on datasets C and D. The horizontal bar within the boxes depicts the median; upper and lower edges of the boxes are the upper and lower quartile; the whiskers include 95% of all data; outliers are not depicted

The results differ significantly from datasets A and B. The Stribeck and GMS are both able to model the frictional effects. Both suffer from errors due to positional effects, which are more significant on the y-axis due to the longer distance. The RE on the test datasets are around 10% higher on the y-axis than on the x-axis. The differences between training and test datasets are small, showing that the models do not overfit.

The data-based models SVR and GMSSVR show different behavior. The SVR model performs well on the training datasets of both axis, however, showing high errors of up to 51.3% on the test dataset. This is a sign for overfitting of the model, showing that it is not capable of generalizing well on the given data.

Only the GMSSVR model is able to model the positional effects as well on both axes and establishes significantly lower errors on nearly all datasets than the other models.

Table 4. RMSE and RE of all on datasets A,B,C and D (significant positional effect)

Dataset	Metric	X-axis				Y-axis			
		STRIBECK	SVR	GMS	GMSSVR	STRIBECK	SVR	GMS	GMSSVR
A+B (Training)	RMSE (in A)	0.12	0.11	0.10	0.08	0.29	0.07	0.29	0.16
	RE (in %)	10.3	9.2	8.9	6.6	23.2	5.5	23.0	12.0
C+D (Testing)	RMSE (in A)	0.12	0.50	0.13	0.08	0.32	0.64	0.31	0.15
	RE (in %)	10.1	42.2	11.0	7.1	25.3	51.3	25.0	12.0

The performance of all models in time domain is further depicted in Fig. 6. The Stribeck and GMS model are only averaging effects along different positions, while the SVR is performing poor on the whole dataset. Regarding the GMSSVR, it shows small errors only at the end of the workspace, and performs very well at other locations. The model shows its capability on modeling friction on both axis over nearly full range of motion.

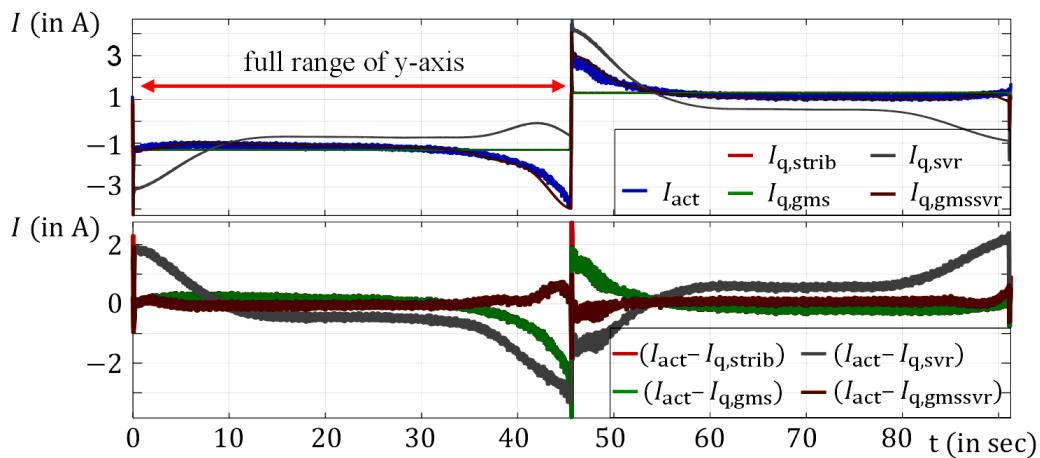


Fig. 6. Comparison of the different models on y-axis in time domain on dataset D (significant positional effect)

6. CONCLUSION

This work shows a new grey box approach to model frictional effects of machine tool auxiliary drives with significant positional influences on the friction. Classic static and dynamic friction models are unable to cover those positional effects. The proposed model utilizes the well-established GMS friction model and combines it with a data-based approach, namely a SVR, to a GMSSVR model. The new approach was evaluated with known friction models, GMS and Stribeck and as well as a sole data-based SVR model. While the classic friction models are able to perform well on a dataset without positional effects, where the axes are only moved in a small area in the middle of their working ranges, the errors get high on the full range of motion of the axes. Only the GMSSVR model is able account for the positional effects as well, which allows a correction of frictional effects with little error. Further improvements could be established by providing a bigger dataset.

ACKNOWLEDGEMENTS

The presented research was funded by the Deutsche Forschungsgemeinschaft (DFG, German Research Foundation) - 497676155.

REFERENCES

- [1] STEMMLER S., ABEL D., SCHWENZER M., ADAMS O., KLOCKE F., 2017, *Model Predictive Control for Force Control in Milling*, IFAC-PapersOnLine, 50/ 1, 15871–15876.
- [2] SCHWENZER M., STEMMLER S., AY M., RÜPPEL A.K., BERGS T., ABEL D., 2022, *Model Predictive Force Control in Milling Based on an Ensemble Kalman Filter*, Journal of Intelligent Manufacturing, 33/7, 1907–1919.
- [3] LEE W., LEE C.-Y., JEONG Y.H., MIN B.-K., 2015, *Friction Compensation Controller for Load Varying Machine Tool Feed Drive*, International Journal of Machine Tools and Manufacture, 96, 47–54.
- [4] RAFAN N.A., JAMALUDIN Z., CHIEW T.H., ABDULLAH L., MASLAN M.N., 2015, *Contour Error Analysis of Precise Positioning for Ball Screw Driven Stage Using Friction Model Feedforward*, Procedia CIRP, 26, 712–717.
- [5] YANG M., YANG J., DING H., 2018, *A Two-Stage Friction Model and its Application in Tracking Error Pre-Compensation of CNC Machine Tools*, Precision Engineering, 51, 426–436.
- [6] BUI B.D., UCHIYAMA N., SANO S., 2015, *Nonlinear Friction Modeling and Compensation for Precision Control of a Mechanical Feed-Drive System*, Sensors and Materials, 27/10, <https://doi.org/10.18494/SAM.2015.1134>.
- [7] ARMSTRONG-HELOUVRY B., DUPONT P., de WIT C.C., 1994, *A Survey of Models, Analysis Tools and Compensation Methods for the Control of Machines with Friction*, Automatica, 30/7, 1083–1138, [https://doi.org/10.1016/0005-1098\(94\)90209-7](https://doi.org/10.1016/0005-1098(94)90209-7).
- [8] COULOMB C.A., 1785, *Theorie des Machines Simples, en Ayant Egard au Frottement de Leurs Parties, et a la Roideur Dews Cordages*, Mémoires de Mathématique et de Physique, x, 161–342.
- [9] REYNOLDS O., 1886, *IV. on the Theory of Lubrication and its Application to Mr. Beauchamp Tower's Experiments, Including an Experimental Determination of the Viscosity of Olive Oil*, Philosophical Transactions of the Royal Society of London, 177, 157–234.
- [10] SOMMERFELD A., 1904, *Zur Hydrodynamischen Theorie der Schmiermittelreibung*, Zeitschrift für Mathematik und Physik, 50, 97–155.
- [11] HERSEY M.D., 1914, *The Laws of Lubrication of Horizontal Journal Bearings*, Journal of the Washington Academy of Sciences, 4/19, 542–552.

- [12] STRIBECK R., 1902, *Die wesentlichen Eigenschaften der Gleit- und Rollenlager*, Zeitschrift des Vereines Deutscher Ingenieure, 46, 1341–1348.
- [13] DAHL P.R., 1968, *A Solid Friction Model*, Technical rept. Published by Aerospace Corp. el segundo CA, <https://apps.dtic.mil/sti/citations/ADA041920>, last checked: 20.01.2024.
- [14] RABINOWICZ E., 1958, *The Intrinsic Variables Affecting the Stick-Slip Process*, Proceedings of the Physical Society, 71/4, 668–675.
- [15] HESS D.P., SOOM A., 1991, *Normal Vibrations and Friction Under Harmonic Loads: Part I—Hertzian Contacts*, Journal of Tribology, 113/1, 80–86.
- [16] CANUDAS DE WIT C., OLSSON H., ASTROM K.J., LISCHINSKY P., 1995, *A New Model for Control of Systems with Friction*, IEEE Transactions on Automatic Control, 40/3, 419–425.
- [17] SWEVERS J., AL-BENDER F., GANSEMAN C.G., PROJOGO T., 2000, *An Integrated Friction Model Structure with Improved Presliding Behavior for Accurate Friction Compensation*, IEEE Transactions on Automatic Control, 45/4, 675–686.
- [18] AL-BENDER F., LAMPAERT V., SWEVERS J., 2005, *The Generalized Maxwell-Slip Model: a Novel Model for Friction Simulation and Compensation*, IEEE Transactions on Automatic Control, 50/11, 1883–1887.
- [19] SCHWENZER M., AUERBACH T., MIURA K., DÖBBELER B., BERGS T., 2020, *Support Vector Regression to Correct Motor Current of Machine Tool Drives*, Journal of Intelligent Manufacturing, 31/3, 553–560.
- [20] BOSER B.E., GUYON I.M., VAPNIK V.N., 1992, *A Training Algorithm for Optimal Margin Classifiers*, Haussler, D. (Hrsg.): Proceedings of the Fifth Annual Workshop on Computational Learning Theory, Pittsburgh Pennsylvania USA, 27 07 1992–29 07 1992. New York, NY, USA, ACM, 144–152.
- [21] VAPNIK V., GOLOWICH S., SMOLA A., 1996, *Support Vector Method for Function Approximation, Regression Estimation and Signal Processing*, Mozer M.C., Jordan M., Petsche T., (Hrsg.), Advances in Neural Information Processing Systems, 9, NeurIPS Proceedings.
- [22] KIM G.D., CHU C.N., 1999, *Indirect Cutting Force Measurement Considering Frictional Behaviour in a Machining Centre Using Feed Motor Current*, The International Journal of Advanced Manufacturing Technology, 15/7, 478–484.
- [23] FUJITA T., XI T., IKEDA R., KEHNE S., FEY M., BRECHER C., 2022, *Identification of a Practical Digital Twin for Simulation of Machine Tools*, International Journal of Automation Technology, 16/3, 261–268.
- [24] HONG Y.-C., HA S.-J., CHO M.-W., 2012, *Predicting of Cutting Forces in a Micromilling Process Based on Frequency Analysis of Sensor Signals and Modified Polynomial Neural Network Algorithm*, International Journal of Precision Engineering and Manufacturing, 13/1, 17–23.
- [25] SHINNO H., HASHIZUME H., YOSHIOKA H., 2003, *Sensor-less Monitoring of Cutting Force during Ultraprecision Machining*, CIRP Annals, 52/1, 303–306.
- [26] AUCHET S., CHEVRIER P., LACOUR M., LIPINSKI P., 2004, *A New Method of Cutting Force Measurement Based on Command Voltages of Active Electro-Magnetic Bearings*, International Journal of Machine Tools and Manufacture, 44/14, 1441–1449.
- [27] DENKENA B., HACKELO F.L., 2010, *Multi-sensor Disturbance Force Measurement for Compliant Mechanical Structures*, IEEE Sensors, Kona, HI, 01.11.2010–04.11.2010, IEEE, 2518–2524.
- [28] MIURA K., BERGS T., 2019, *A Method of Cutting Power Monitoring for Feed Axes in Milling by Power Measurement Device*, IFAC-PapersOnLine, 52/13, 2471–2476.
- [29] YAMADA Y., KAKINUMA Y., 2016, *Sensorless Cutting Force Estimation for Full-Closed Controlled Ball-Screw-Driven Stage*, The International Journal of Advanced Manufacturing Technology, 87/9–12, 3337–3348.
- [30] YAMADA Y., YAMATO S., KAKINUMA Y., 2017, *Mode Decoupled and Sensorless Cutting Force Monitoring Based on Multi-Encoder*, The International Journal of Advanced Manufacturing Technology, 92/9-12, 4081–4093.
- [31] XI T., FUJITA T., KEHNE S., IKEDA R., FEY M., BRECHER C., 2022, *An Extended LuGre Model for Estimating Nonlinear Frictions in Feed Drive Systems of Machine Tools*, Procedia CIRP, 107, 452–457.
- [32] CARLSON F.B., ROBERTSSON A., JOHANSSON R., 2015, *Modeling and Identification of Position and Temperature Dependent Friction Phenomena Without Temperature Sensing*, 2015, IEEE/RSJ International Conference on Intelligent Robots and Systems (IROS), Hamburg, Germany, 28.09.2015–02.10.2015, IEEE, 3045–3051.
- [33] TJAHJOWIDODO T., AL-BENDER F., VAN BRUSSEL H., SYMENS W., 2007, *Friction Characterization and Compensation in Electro-Mechanical Systems*, Journal of Sound and Vibration, 308/3–5, 632–646.
- [34] ZSCHACK S., BUCHNER S., AMTHOR A., AMENT C., 2012, *Maxwell Slip Based Adaptive Friction Compensation in High Precision Applications*, IECON 2012 – 38th Annual Conference on IEEE Industrial Electronics Society, Montreal, QC, Canada, 25.10.2012–28.10.2012, IEEE, 2331–2336.